Whereas the integrals Eqs. (29) and (32) are used here to develop force and moment expressions, some analysts use linear combinations of z evaluated at discrete points. Regardless of which approach is used, the series representation leads to a frequency response of torque to swivel angle, $G_{M\psi}(j\omega)$, in which the coefficient of the $j\omega$ term in the numerator is zero and higher terms are not zero. This occurs because the coefficient of $s\bar{\psi}$ in Eq. (A2) is zero. When one of the coefficients of a polynomial is zero, there are either pure imaginary roots or roots with positive real parts. The polar plot of $G_{M\psi}(j\omega)$ starts on the positive real axis for ω equal to zero, moves clockwise toward the origin as ω increases, passes near the origin, and continues toward the positive real axis. For a conjugate pair of pure imaginary zeros, the plot passes through the origin; for a conjugate pair of zeros with positive real parts, the plot circles the origin. (Segel's circles the origin.) From physical consideration of phase angles at high frequencies, the plot must not circle the origin.

The approach of $G_{M\psi}(j\omega)$ to the origin is seen to be crucial. The string model is inadequate to yield the correct results on this sensitive point, although it does indicate a close approach to the origin and yields the proper characteristics of the remaining frequency responses. The effect of the ε term in the theory of the paper is to cause $G_{M\psi\varepsilon}(j\omega)$ not to pass through or to circle the origin.

The denominators of Eqs. 23, A1 and A2) roughly correspond to characteristic functions [see Eqs. (31) and (34)]. Comparing Eqs. (A1) and (A2) it is seen that the polynomial approximates the exponential, which has no roots. With this and the above paragraphs in mind, it is not surprising that some shimmy investigators have found that truncations of the series can introduce spurious roots.

References

[1] Rogers, L. C. and Brewer, H. K., "Synthesis of Tire Equations for Shimmy and other Dynamic Studies," *Journal of Aircraft*, Vol. 8, No. 9, Sept. 1971, pp. 689–697

[2] Collins, R. L. and Black, R. J., "Tire Parameters for Landing-Gear Shimmy Studies," *Journal of Aircraft*, Vol. 6, No. 3, May-June 1969, pp. 252–258.

[3] Pacejka, H. B., "The Wheel Shimmy Phenomenon," Ph.D. thesis, 1966, Delft Technical Institute, Delft, Holland.

[4] Collins, R. L., "Theories on the Mechanics of Tires and Their Applications to Shimmy Analysis," *Journal of Aircraft*, Vol. 8, No. 4, April 1971, pp. 271–277.

[5] Brewer, H. K., "Cornering Force and Self-Aligning Torque Response of a Tire Undergoing Sinusoidal Variations in Steer Angle," Rept. Nov. 1965, B. F. Goodrich Research Center, Brecksville, Ohio.

[6] Segel, L., "Force and Moment Response of Pneumatic Tires to Lateral Motion Inputs," *Transactions of the ASME, Journal of Engineering for Industry*, 88B, 1966, 1, 8 p.; also Paper 65-Av-2.

[7] Smiley, R. F., "Correlation, Evaluation, and Extension of Linearized Theories for Tire Motion and Wheel Shimmy," Rept. 1299, 1957, NACA.

[8] Smiley, R. F. and Horne, W. B., "Mechanical Properties of Pneumatic Tires with Special Reference to Modern Aircraft Tires," TR-R-64, 1960, NASA.

AUGUST 1972 J. AIRCRAFT VOL. 9, NO. 8

Combined Viscous-Inviscid Analysis of Supersonic Inlet Flowfields

THEODORE A. REYHNER* AND TIMOTHY E. HICKCOX†

The Boeing Company, Seattle, Wash.

A procedure is described for analytically predicting the flowfield in the supersonic diffuser of a supersonic inlet. It differs from existing techniques which calculate the inviscid flow in the inlet independent of the viscous flow by calculating the effects of the viscous flow on the inviscid flowfield of the inlet. The procedure consists of first calculating the inviscid flow without viscous effects. Then the boundary-layer growth in the inlet including bleed, bleed scoops and shock wave/boundary-layer interactions is calculated. A second inviscid flow calculation is then made which is matched to the boundary-layer solution. The various steps of the procedure are described with emphasis on the matching of the viscous (boundary layer) and inviscid solutions. Comparisons of predictions with experiments for a Mach 3.0 and a Mach 2.65 mixed-compression supersonic inlet show that this procedure accurately predicts the inlet flowfields and that the effects of the boundary layer on the flowfield are very significant.

Nomenclature

$\dot{m}_{BL}$ = bleed mass flow
$\dot{m}_{139}$ = bleed mass flow used for boundary-layer computation
n = coordinate normal to inlet surface
p_p = Pitot probe pressure
p_s = static pressure
R = distance from surface to inlet axis
R_L = radius of inlet lip
u = velocity component parallel to surface
X = coordinate along inlet axis
δ^* = boundary-layer displacement thickness,

$$\int_0^{\delta}\left(1-\frac{\rho u}{\rho_e u_e}\right)dn$$

δ^*_{BL} = bleed equivalent displacement thickness, $(\dot{m}_{BL}/\rho_e u_e 2\pi R)$ (axisymmetric inlet)
δ = boundary-layer thickness
η = bleed efficiency parameter
ρ = density

Presented as Paper 72-44 at the AIAA 10th Aerospace Sciences Meeting, San Diego, Calif., January 17–19, 1972; submitted January 27, 1972; revision received May 8, 1972.

Index categories: Subsonic and Supersonic Airbreathing Propulsion; Jets, Wakes and Viscid-Inviscid Flow Interactions.

* Senior Engineer, Commercial Airplane Group. Member AIAA.

† Engineer, Commercial Airplane Group.

Subscripts

e = outer edge of boundary layer
T = stagnation conditions
∞ = freestream conditions

Introduction

In the past, supersonic inlet flowfields were analyzed only with inviscid flow calculation procedures. This was done because methods to account analytically for viscous effects did not exist. Criteria based on consideration of viscous flow effects were used with the inviscid flow program results to select inlet contours. These criteria included empirical results on shock strength causing boundary-layer separation and the intuition of the designer as to the severity of adverse pressure gradients which would cause separation. Because the analysis did not predict viscous flow effects, an extensive series of tests was required to develop a boundary-layer control system and made necessary contour modifications. For the Boeing SST program, the design procedure was significantly improved by using the inviscid flow predictions to calculate boundary-layer development in the inlet. A bleed system was then designed on the basis of the predicted boundary-layer growth. Modifications to the contours were made if boundary-layer predictions showed that they would be desirable.

This design procedure still did not account for the changes in the inviscid flow due to the boundary layer. The boundary layer causes the shock system and pressure gradients in the inlet to be displaced from the predicted inviscid location. Shock wave/boundary-layer interactions can also give rise to complex systems of shocks and expansion waves. Mass removal for boundary-layer control leads to further changes in the flowfield. The net effect is that the original analytic boundary-layer predictions are not accurate and thus the analytic bleed-system design is not optimum. The severity of these problems increases with increasing Mach number because the boundary layer becomes thicker relative to the over-all flowfield. A further problem occurs because most testing involves small models tested at other than flight Reynolds numbers. A better way of predicting viscous effects thus is required to extrapolate model test results to flight conditions. Now, a procedure for combining viscous and inviscid analysis of supersonic inlet flowfields has been developed called "The Combined Flowfield Analysis" to provide an improved inlet and bleed-system design method by accounting for viscous effects on the inviscid flowfield.

Selection of Approach

The Combined Flowfield Analysis is based on the use of existing computer programs with only minor modifications. There are several possible ways of including the viscous effects on the inviscid flow in a supersonic inlet. The ultimate approach would be a complete solution of the flowfield using an asymptotic solution of time-dependent equations. This was, and is, unfeasible from both cost and time-schedule viewpoints. The only practical approach appeared to be matching of existing boundary layer and inviscid flow solutions. Both the boundary layer and method of characteristics solutions have the property that the computations progress in the direction of the flow. This suggested three posssibilities: 1) that the solutions be marched simultaneously; 2) that one solution and then the other be computed to the end of the supersonic flow region; or 3) that the flowfield be divided into subregions and that the solution be completed for the flowfield in one subregion before going on to the next subregion. A computation from shock wave/boundary-layer interaction to shock wave/boundary-layer interaction would be a natural choice for a calculation by subregions. The first method was ruled out because of the possibility that the solution might diverge towards strong-interaction solutions instead of the desired weak-interaction solution‡ and because it would have to be done entirely with one computer program and thus would involve a lengthy programming effort.

The subregion-to-subregion approach was feasible and as a technique for the future has several advantages. If the calculation was done from shock interaction to shock interaction each shock wave/boundary-layer interaction has only to be computed once. If a very sophisticated interaction analysis is developed this would be a real cost-saving feature. Iteration can be completed for each subregion before continuing on to the next. This should speed convergence because not as much of the flowfield is being changed, and with no shock interactions in the subregion, changes in surface pressure will be small. However, a subregion-to-subregion procedure with separate viscous and inviscid flow programs would take a great deal of time for each flowfield determination because of the time required for data preparation, submission of computer runs, and preparation of data for the next segment. This approach was eliminated because it was not practical without combining the existing computer programs into a single program.

The choice for the immediate effort was to calculate the entire flowfield with the inviscid flow program and then calculate the boundary-layer growth through the entire inlet. Then a modified inviscid solution was calculated. Many of the techniques developed for this procedure could be used in the development of a subregion-by-subregion calculation.

Viscous Layer Analysis

The boundary-layer program used for the Combined Flowfield Analysis is based on Boeing Computer Program TEM139,[2] a finite-difference solution of the boundary-layer equations. TEM139 computes laminar and turbulent boundary-layer development on two-dimensional or axisymmetric surfaces with or without heat transfer. The program handles regions of bleed or blowing. Transition may be specified as occurring at a given location or at a given momentum-thickness Reynolds number.

The program uses the method of TEM139 to calculate the growth of the boundary layer across segments. Segments are separated by bleed scoops and oblique shock wave/turbulent boundary-layer interactions. The program input and output formats are designed to minimize the amount of hand calculations needed for the complete Combined Flowfield Analysis.

There are two ways mass can be removed in the boundary-layer computations. TEM139 includes an analysis which corresponds to a smooth porous wall. The other way is with a sharp-edged scoop parallel to the wall. The program truncates the boundary-layer profile at the height of the scoop (Fig. 1) and continues calculating with the remaining portion of the profile.

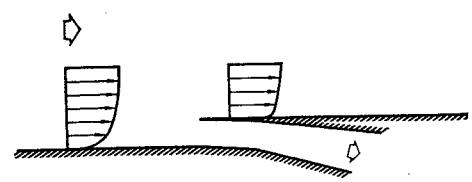

Fig. 1 Boundary-layer scoop.

‡ A strong interaction is the phenomena of shock wave/boundary-layer interaction or flow in corners which have been solved by simultaneous solution of the boundary-layer equations with an inviscid flow matching boundary condition.[1]

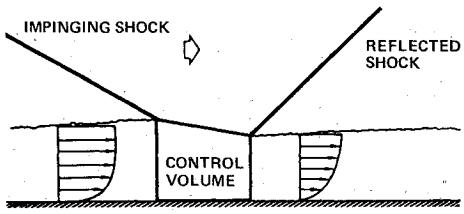

Fig. 2 Integral oblique shock wave/turbulent boundary-layer interaction model.

The oblique shock wave/turbulent boundary-layer interaction analysis is a control-volume analysis (Fig. 2.) This analysis was chosen because it provides good results and was readily available. The upstream profile from the boundary-layer program is fitted by a law-of-the-wall/law-of-the-wake profile.[3] The downstream wall/wake profile is obtained by applying conservation of mass and momentum. The pressure and flow conditions across the shocks come from the inviscid flow solution. The boundary-layer computation is restarted using the downstream profile. The analysis ignores shear forces on the wall for the control volume, entrainment into the boundary layer through the interaction, and assumes a single reflected shock at the downstream end of the interaction.

Inviscid Flow Analysis

The Combined Flowfield Analysis requires a complex yet flexible inviscid flow solution. It must be possible to stop and restart the inviscid flow with altered starting conditions to account for cowl lip leading-edge bluntness. Mass must be removed from the inviscid solution to properly account for bleed. Extremely complex flowfields with intersections of like and opposite family shocks and multiple slip lines will be encountered as a result of disturbances from boundary-layer growth and bleed regions. The inviscid flow solution must be capable of computing these flowfields. Further, flexible definition of surface contours is required.

The Boeing Company has developed the MOCHA (Method Of Characteristics) program, which is a generalized program for the solution of complex supersonic flowfields. The program will compute two-dimensional or axisymmetric, rotational flowfields with multiple shocks. The complete solution of intersection of like and opposite family shocks is included, as well as shock reflections, shocks or expansions from boundary corners; pressure boundaries with separation, reattachment, and intersections with shocks; and the coalescence of Mach lines to form an imbedded shock. The capability to divide or join streams is also included.

The MOCHA program will compute the flowfields encountered in an inlet, handle mass removal at bleed regions, may be restarted as desired, and includes a geometry definition package that is quite flexible. It incorporates all the features required in the Combined Flowfield Analysis. Mass removal from the inviscid solution occurs by means of flow splits. Thus mass removal from a region of continuous bleed must be represented by a scoop in the characteristics solution. The program has internal plotting routines which produce plots of characteristics, slip lines, shocks, and boundaries for easy flowfield visualization.

Combined Flowfield Analysis

The basic procedure for the Combined Flowfield Analysis is: first, the inviscid flow program MOCHA is used to calculate the supersonic flowfield including the effect of cowl lip bluntness for the given inlet contours; second, the Mach number distribution on the surfaces from the characteristics solution along with a bleed distribution is used as input to the boundary-layer program to compute the boundary-layer development through the supersonic diffuser; third the contours of the inlet are modified by the computed boundary-layer displacement thickness. Mass removal for both scoops and bleed regions is represented by scoops for MOCHA. Discontinuities in the modified contour such as those due to the shock wave/turbulent boundary-layer interaction or the transition model are smoothed. The resulting displaced contours along with the correction for cowl lip bluntness are used to calculate a second MOCHA solution.

The initial step in the procedure is to determine the inviscid flowfield based on the original contour. If the cowl lip has leading-edge bluntness, the cowl lip shock is displaced in position and inclined at the cowl lip plane based on the analysis of Moeckel.[4] The cowl surface conditions are taken to be the same as for an attached shock, as the high entropy air on the surface is rapidly entrained in the boundary layer. (The blunt body shock layer for most supersonic mixed-compression inlets is thin because the cowl lip is made as sharp as is practical. This assumption would not be valid for massive lip bluntness.)

Using the predicted surface conditions, known bleed regions and bleed quantities, the boundary-layer development is predicted for both cowl and centerbody. A new displaced contour is defined for both surfaces at the boundary-layer displacement thickness. This displacement-thickness surface defines an "effective" surface for the inviscid core flow. In bleed regions an equivalent δ^*_{BL} based on the cumulative mass removed is computed

$$\delta^*_{BL} = \dot{m}_{BL}/\rho_e u_e 2\pi R \text{ (axisymmetric inlet)} \qquad (1)$$

This "bleed displacement thickness" indicates an effective increase in the flow area for the upstream inviscid core. It therefore has opposite sign from δ^* when displacing the contour. At the end of the bleed region the displaced contour returns to the boundary-layer displacement thickness. This step jump forms the scoop used for mass removal in the inviscid flow. The bleed region then appears to the inviscid flow as an expansive ramp followed by a mass removal scoop (Fig. 3). In a region of distributed wall bleed, the new effective surface may cross the real surface, just as streamlines in the real flow cross the wall in a bleed region.

Comparisons of experimental and theoretical results at The Boeing Company have shown that the effects of bleed on the boundary layer are very sensitive to the way the bleed is removed from the boundary layer. The porous wall model of the computer program produces results very similar to those for a bleed scoop. Boundary-layer profile improvement by bleed removal through holes approaches the scoop results as a limit. Frequently, due to other considerations, the ratio of bleed hole diameter to the boundary-layer displacement thickness is large. In this case, the bleed holes act as a significant roughness and tend to thicken the boundary layer which offsets the thinning effect of mass removal. This effect is corrected for through the use of empirical results. In the boundary-layer calculations less bleed than is actually removed is used in order that the boundary-layer height after the bleed region be closer to that measured. The bleed

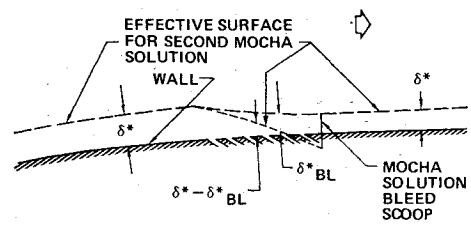

Fig. 3 Procedure for calculating Combined Flowfield solution across bleed regions.

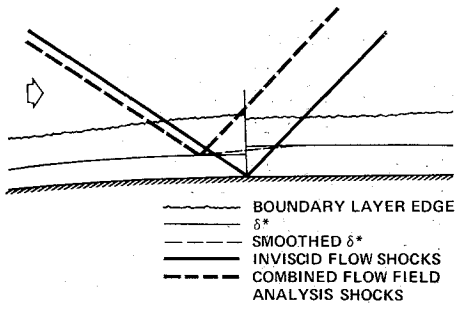

Fig. 4 Procedure for handling oblique shock wave/turbulent boundary-layer interactions.

scoop for the MOCHA run is adjusted to represent the actual mass removed

$$\dot{m}_{139} = \eta \dot{m}_{BL} \tag{2}$$

where $\dot{m}_{139}$ is the mass removed in the boundary-layer program calculation and η is the empirically determined bleed efficiency $0 < \eta \leq 1$. Across the bleed region the surface is displaced $\delta^* - \delta^*_{BL}$ from the actual surface.

This new inlet contour then provides a new "effective" supersonic diffuser. Based on this new contour a new inviscid flow solution is computed. Cowl lip bluntness is accounted for in the same manner as initially. Oblique shock wave/boundary-layer interactions tend to move the reflected shock upstream of the inviscid prediction. Work done at Boeing indicates that for relatively thin boundary layers this movement can be approximated by reflecting the shock wave from the displacement-thickness modified surface. Thus, in the Combined Flowfield solution the oblique shocks are simply reflected from the effective surface (Fig. 4). When the results of the interaction analysis (Fig. 2) are used the length of the interaction zone is neglected. This is done because the model is only approximate. As a result the calculated displacement surface is discontinuous at the interaction. The effective surface in this region is generated by smoothing the displacement-thickness surface to eliminate the discontinuity. The ramp scoops formed in the displaced contour across bleed regions provide mass removal from the inviscid solution. (Across the bleed region the effective area growth is accounted for by the bleed scoop ramp. The real mass flow per unit area is accounted for downstream of the bleed region by removing mass from the inviscid core and returning to the boundary-layer displacement thickness as the effective contour of the inviscid flow.) The bleed effect is well simulated, with surface pressure relief across the bleed region and a return to higher surface pressure at the termination of bleed.

The present method used by the boundary-layer program for handling transition from laminar to turbulent flow calculates an abrupt decrease in δ^* at transition. Smoothing is used to remove this dip in the effective surface to avoid difficulties with the inviscid flow calculation.

A principle problem and the main obstacle to making the Combined Flowfield Analysis into a single computer program is preparing the modified boundary such that it is acceptable to MOCHA. MOCHA is a supersonic flow program and as such cannot handle any regions of subsonic flow. There are certain properties that the boundary must have in order that the characteristics solution not be stopped by a local region of Mach one flow. If the boundary is wavy, shocks may be generated near the surface with attendant total pressure loss. In the far field these shocks will attenuate, but near the wall they will cause a region of high entropy which is much more likely to become subsonic. If the second MOCHA solution is to be computed any distance into the inlet it is essential that the results of the boundary-layer program be carefully prepared.

The smoothing is not too difficult when this part of the analysis is done by hand, but it would be much more difficult to write a computer program to do it in a consistent manner. On first glance the problem of smoothing may appear simple, but in reality it requires a great deal of judgement. The engineer knows what is physically meaningful and what is a peculiarity of the solution procedure that can quite reasonably be ignored. As an example, for the region at the inlet throat and downstream of the throat a typical characteristics solution shows frequent shocks and strong pressure gradients. Due to cummulative viscous effects, the real pressure distribution will be quite different and it is reasonable to do considerable smoothing of the calculated boundary-layer displacement thickness.

A unique possibility arises which cannot be bypassed in the Combined Flowfield Analysis. That is the possibility of a portion of the flow within the boundary layer becoming subsonic at an oblique shock reflection. The result would be a small-scale lambda shock structure. If the resulting subsonic region extends outside δ^*, the Combined Flowfield Analysis will go subsonic at the shock reflection. This will terminate the method of characteristics solution. This is an unfortunate, but presently unavoidable, problem. Any subsonic pockets in the flow will stop the characteristics solution even though they may be small and of no significance with regard to the real flowfield.

Results

Two applications of the Combined Flowfield Analysis are presented to illustrate the capabilities of the analysis. The results of the Combined Flowfield Analysis and a strictly inviscid prediction for inlet flowfields are compared with data for a Mach 3.0 (Ref. 5) and a Mach 2.65 (Ref. 6) inlet, both operating at their design Mach numbers. For both inlets boundary-layer growth predictions are compared with experiment, and the Combined Flowfield Analysis and inviscid flow predictions for surface static pressure are compared with measurements. For the Mach 2.65 inlet, the difference in the predicted shock locations between the strictly inviscid flow calculation and the Combined Flowfield Analysis is shown. Performance of the Mach 2.65 inlet had previously been estimated[7] using the techniques discussed in this paper except for the final step of calculating the Combined Flowfield Solution.

Mach 3.0 Inlet

The first case is the Mach 3.0 design point inlet. This is a mixed-compression, axisymmetric inlet, with isentropic external centerbody compression. The results of the boundary-layer profile predictions ahead of and behind the bleed regions in the supersonic diffuser are compared with data in Fig. 5. The upstream profiles agree quite well with the data. The downstream profile agreement is not as good.

There are several problems with predicting the boundary-layer growth in this inlet that primarily affect the prediction of the downstream profile. The diameter of the bleed holes in the inlet is 0.125 in. The boundary-layer thickness predicted is on the order of 0.1 to 0.2 in. The holes are very large relative to the boundary layer and thus have a significant roughness effect which is difficult to predict. The bleed efficiency factor η used to correct for this effect was 0.5. The boundary-layer measurements were made for maximum recovery operation. This means that the normal shock was very near the throat of the inlet and that the effects of the normal shock probably fed forward through the subsonic part of the boundary layer to the vicinity of the aft boundary-layer profile. At present no method is available to predict detailed structure of the boundary layer when it is in the region of influence of the normal shock.

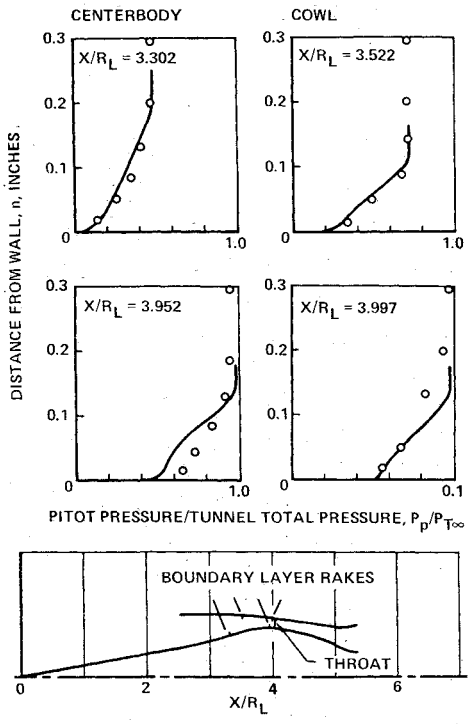

Fig. 5 Comparison of predicted boundary layer with experimental results (Ref. 5, $M_\infty = 3.0$).

Comparisons for the centerbody and cowl surface pressure distributions are shown in Figs. 6 and 7, respectively. The Combined Flowfield Analysis included a very small bluntness effect. The Combined Flowfield Analysis gives significantly improved agreement with the data as compared to the inviscid flowfield predictions. In particular, the Combined Flowfield Analysis shows the increased pressure and pressure gradient behind the first centerbody shock reflection (Fig. 6). In addition, the points in the first centerbody bleed region greatest improvement in cowl surface pressure agreement with data (Fig. 7) occurs behind the first cowl bleed region and the first cowl shock reflection. Significantly higher surface pressures exist here than predicted by the inviscid analysis. The experimental points labeled "normal shock forward" correspond to the inlet mode of operation when the boundary-layer profiles were measured. As can be seen, they correspond much more closely to the data. The centerbody solution terminates because subsonic flow was calculated at about the same station on the cowl as shown in Fig. 7. The measured pressures are higher near the location where the downstream boundary-layer profiles were measured which indicates that the normal shock is affecting the surface pressure distribution. The Combined Flowfield Analysis predictions correspond to the normal shock aft. Subsonic flow is

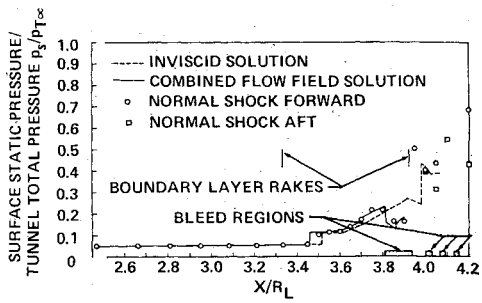

Fig. 6 Comparison of analytic predictions with experiment for centerbody static pressure distribution (Ref. 5, $M_\infty = 3.0$).

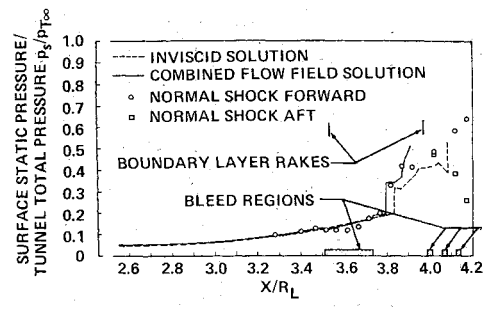

Fig. 7 Comparison of analytic predictions with experiment for cowl static pressure distribution (Ref. 5, $M_\infty = 3.0$).

predicted on the cowl surface, downstream of the first cowl shock reflection in a region of strong adverse pressure gradient. The significance of the predicted flow becoming subsonic is not known. The data shows that the flow was close to Mach one in the experiment. It is possible for a small subsonic pocket to exist in a transonic flow, or it is possible that the problem is a slight inaccuracy in the computation that happens to be in the direction of subsonic flow.

Mach 2.65 Inlet

The second case is the Mach 2.65 design point inlet. It is also a mixed-compression axisymmetric inlet. The results of the boundary-layer predictions are compared with data in Fig. 8. The boundary-layer growth predictions for both

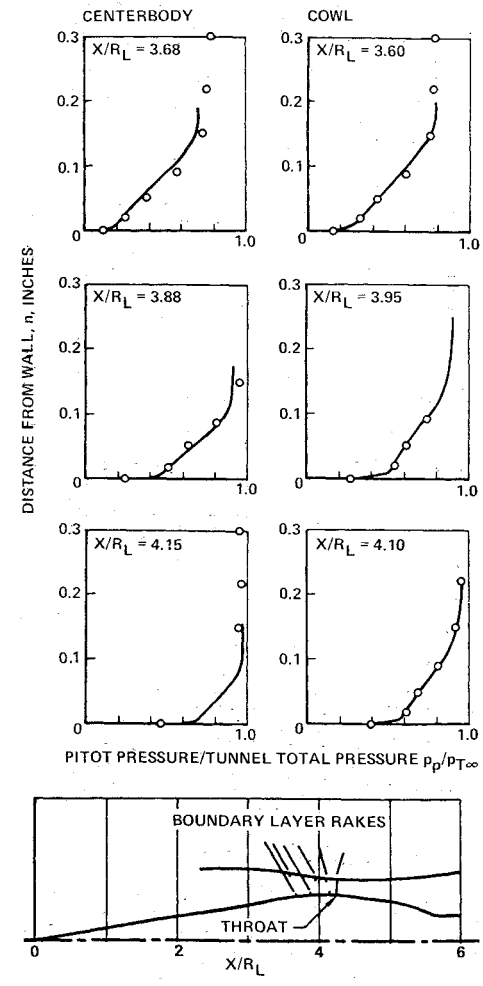

Fig. 8 Comparison of predicted boundary layer with experimental results (Ref. 6, $M_\infty = 2.65$, configuration 22).

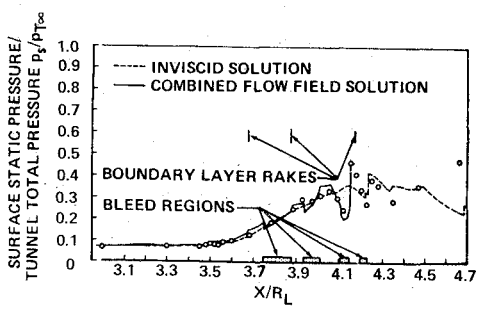

Fig. 9 Comparison of analytic predictions with experiment for centerbody static pressure distribution (Ref. 6, $M_\infty = 2.65$, configuration 22).

the centerbody and cowl are in very close agreement with experimental results. This is particularly significant as the profiles occur ahead of any shock interaction or bleed, following a single bleed region and shock reflection, and finally following multiple bleed regions and shock/boundary-layer interactions.

The bleed-hole diameter for this inlet was 0.0625 in. and the boundary-layer thickness was also of the order of 0.1–0.2 in. The forward most holes were inclined at 20° to the surface, the next holes at 40°, and the aft holes at 90°. Work at Boeing has shown that both the smaller holes plus the inclination of the holes will lead to improved bleed efficiency. The predictions were made with bleed efficiencies of 0.8, 0.7, and 0.5 for the 20°, 40°, and 90° holes, respectively. Also the test data is for a low recovery mode which means the normal shock is well aft of the throat. This corresponds more closely to the analytic predictions.

The centerbody and cowl surface pressure distributions are shown in Figs. 9 and 10, respectively. The cowl lip was assumed to be sharp (no bluntness correction). There is a marked improvement in agreement with data for the Combined Flowfield Analysis as compared with inviscid analysis. The small pressure rise at the centerbody shock reflection is better predicted by the Combined Flowfield Analysis (Fig. 9).

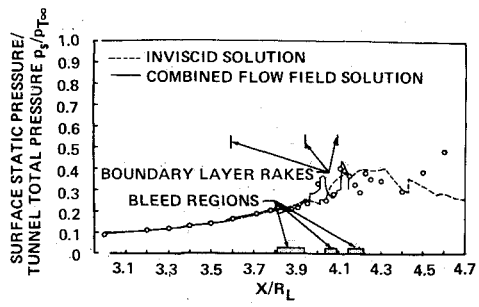

Fig. 10 Comparison of analytic predictions with experiment for cowl static pressure distribution (Ref. 6, $M_\infty = 2.65$, configuration 22).

The centerbody pressure drop and rise ahead of and behind the third bleed region is closely predicted, where it was not in the inviscid analysis. The cowl surface pressure (Fig. 10) shows very good agreement all along the surface. The solution and data match well through the bleed regions, with particularly improved agreement over the inviscid solution between the first and second bleed regions and following the second bleed region. The case terminated because the predicted flow was subsonic at a shock intersection just off the centerbody.

To better illustrate the significance of the Combined Flowfield Analysis, the shock system plus the expansions from the start of the bleed regions are compared with the inviscid shock system for the Mach 2.65 inlet in Fig. 11. Also shown is the inlet surface and the boundary-layer displaced effective surface including the bleed scoops. This figure shows the relatively large forward shift of the shock system due to a relatively small effective surface displacement caused by the boundary layer.

These two cases show a significantly improved agreement with experimental data for the Combined Flowfield Analysis over a strictly inviscid analysis The effects of bluntness and the boundary layer on the flowfield have been accounted for, and these effects have significantly altered the predicted flowfields. The comparisons with experimental results show that the method accurately predicts boundary-layer growth and surface static pressure distribution in supersonic inlets.

Future Work

This analysis was developed as a continuing effort towards a very complete, easy to apply analysis for supersonic inlet flowfields. Problems have been identified which must be overcome before a more complete, easier to use, more accurate procedure can be developed.

The areas where most of the errors in the analysis are generated are in the handling of bleed regions and oblique shock wave/turbulent boundary-layer interactions. It has already been stated that a correction can be applied to account for bleed-system efficiency. Unfortunately, although data clearly shows the magnitude of the problem, it is not possible at present to give more than a rough guess as to what value to give the efficiency factor for a given case. The bleed-system design for the translating centerbody of the SST inlet was such that the plenums behind various rows of bleed holes were open, partly open, or closed, depending on the position of the centerbody. It is known that the boundary-layer growth across a row of open, but not bleeding, holes is greater than that across a smooth wall. Also, for the partly closed plenums, the bleed efficiency is different than if the holes are choked or nearly choked. These effects have not been accounted for in the present analysis. More experimental results are needed to develop corrections for these effects.

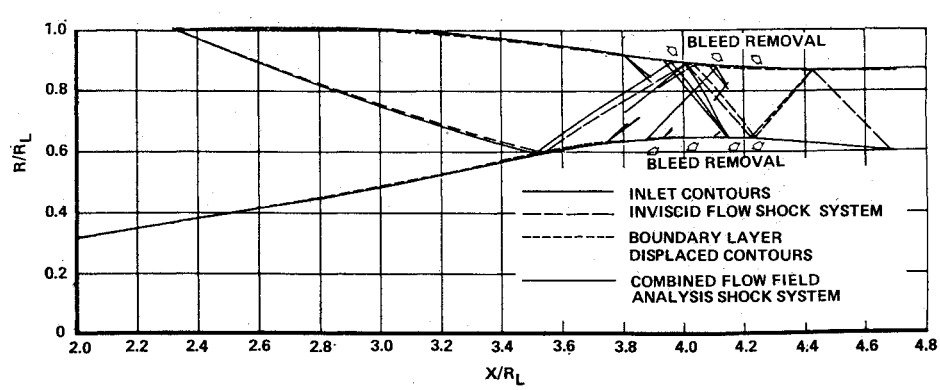

Fig. 11 Comparison between inviscid flow and Combined Flowfield Analysis predictions for shock and expansion wave locations (Ref. 6, $M_\infty = 2.65$, configuration 22).

A better analysis is desired for the oblique shock wave/turbulent boundary-layer interactions. The advantages would include more accurate prediction of the downstream boundary layer, better prediction of the reflected shock structure which is usually a multiple system of shocks and regions of compression and expansion waves, and the capability to handle shocks which are strong enough to cause a local separation of the boundary layer. A very complete analysis also would predict details of the pressure rise along the wall due to the shock wave/boundary-layer interaction which would enhance comparisons of theoretical and experimental results. The shock wave in the combined solution is reflected off the smoothed displacement-thickness surface because that technique was available and fitted the hand combination type of approach. If a detailed analysis for the shock wave/boundary-layer interaction is developed, it will require a machine combined solution since the position of the incident shock is not known in advance of the calculation of the second MOCHA solution.

Cowl lip bluntness is presently approximated as a forward-facing step and solved using Moeckel's method. The solution does not represent the real flowfield in the lip region well, as conditions are only defined at the shock and on the surface. A more accurate method to handle leading-edge bluntness is desirable.

Our goal is eventually to have the entire analysis procedure as a single computer program. At present, no further iterations are made on results because of the time required, and the accuracy in the bleed and shock interaction calculations does not justify iteration. If the analysis were made with a single computer program and some of the approximations were improved, iterations between the viscous flow and inviscid flow solutions would be practical and useful.

Conclusions

A method has been developed which greatly improves the analysis of supersonic diffusers in supersonic inlets. The solution includes the viscous effects and thus provides much improved prediction of the real flowfield as compared to an inviscid solution. This technique predicts the boundary layer and its effect on the inviscid core, including the effects of bleed and shock/boundary-layer interactions. Comparisons with test data have shown significantly improved agreement with the real flowfields.

This procedure is an important advance in the prediction of the real flowfield in a supersonic inlet and provides a basis for further development as our understanding of the problem improves and as improved component analyses become available. This type of technique is particularly important for applications to hypersonic inlets where viscous flow comprises a much larger portion of the flowfield.

References

[1] Reyhner, T. A., "The Interaction of a Shock Wave with a Laminar Boundary Layer," Ph.D. dissertation, Nov. 1966, Stanford Univ., Stanford, Calif.; also abbrev. version, *International Journal of Non-Linear Mechanics*, Vol. 3, No. 2, June 1968, pp. 173–199.

[2] Reyhner, T. A., "A Computer Program for Finite-Difference Calculation of Compressible Turbulent Boundary Layers," D6-23236, 1970, The Boeing Co., Seattle, Wash.

[3] Paynter, G. C. and Schuehle, A. L., "On the Use of Cole's Universal Wake Function for Compressible Turbulent Boundary Layers," D6-22755TN, Nov. 1969, The Boeing Co., Seattle, Wash.

[4] Moeckel, W. E., "Approximate Method for Predicting Form and Location of Detached Shock Waves of Plane or Axially Symmetric Bodies," TN 1921, 1949, NACA.

[5] Smeltzer, D. B. and Sorensen, N. E., "Investigation of a Nearly Isentropic Mixed-Compression Axisymmetric Inlet System at Mach Numbers 0.6 to 3.2," TN D-4557, May 1968, NASA.

[6] Koncsek, J. L. and Syberg, J., "Transonic and Supersonic Test of a Mach 2.65 Mixed-Compression Axisymmetric Intake," CR-1977, March 1972, NASA.

[7] Sorensen, N. E. and Smeltzer, D. B., "Performance Estimates for a Supersonic Axisymmetric Inlet System," AIAA Paper 72-45, San Diego, Calif., 1972.